ORIGINAL ARTICLE

Basic Study

Transcriptional factor III A promotes colorectal cancer progression by upregulating cystatin A

Jing Wang, Yuan Tan, Qun-Ying Jia, Fa-Qin Tang

Jing Wang, Yuan Tan, Qun-Ying Jia, Fa-Qin Tang, Hunan Key Laboratory of Oncotarget Gene, Hunan Cancer Hospital & The Affiliated Cancer Hospital of Xiangya School of Medicine, Central South University, Changsha 410013, Hunan Province, China

Corresponding author: Fa-Qin Tang, MD, PhD, Doctor, Professor, Hunan Key Laboratory of Oncotarget Gene, Hunan Cancer Hospital & The Affiliated Cancer Hospital of Xiangya School of Medicine, Central South University, No. 283 Tongzipo Road, Changsha 410013, Hunan Province, China. tangfq@hnca.org.cn

Abstract

BACKGROUND
Advanced colorectal cancer (CRC) generally has poor outcomes and high mortality rates. Clarifying the molecular mechanisms underlying CRC progression is necessary to develop new diagnostic and therapeutic strategies to improve CRC outcome and decrease mortality. Transcriptional factor III A (GTF3A), an RNA polymerase III transcriptional factor, is a critical driver of tumorgenesis and aggravates CRC cell growth.

AIM
To confirm whether GTF3A promotes CRC progression by regulating the expression of cystatin A (*Csta*) gene and investigate whether GTF3A can serve as a prognostic biomarker and therapeutic target for patients with CRC.

METHODS
Human tissue microarrays containing 90 pairs of CRC tissues and adjacent non-tumor tissues, and human tissue microarrays containing 20 pairs of CRC tissues, adjacent non-tumor tissues, and metastatic tissues were examined for GTF3A expression using immunohistochemistry. The survival rates of patients were analyzed. Short hairpin GTF3As and CSTAs were designed and packaged into the virus to block the expression of *Gtf3a* and *Csta* genes, respectively. *In vivo* tumor growth assays were performed to confirm whether GTF3A promotes CRC cell proliferation *in vivo*. Electrophoretic mobility shift assay and fluorescence *in situ* hybridization assay were used to detect the interaction of GTF3A with *Csta*, whereas luciferase activity assay was used to evaluate the expression of the *Gtf3a* and *Csta* genes. RNA-Sequencing (RNA-Seq) and data analyses were used to screen for target genes of GTF3A.

RESULTS

The expression of GTF3A was higher in CRC tissues and lymph node metastatic tissues than in the adjacent normal tissues. GTF3A was associated with CRC prognosis, and knockdown of the *Gtf3a* gene impaired CRC cell proliferation, invasion, and motility *in vitro* and *in vivo*. Moreover, RNA-Seq analysis revealed that GTF3A might upregulate the expression of *Csta*, whereas the luciferase activity assay showed that GTF3A bound to the promoter of *Csta* gene and increased *Csta* transcription. Furthermore, CSTA regulated the expression of epithelial-mesenchymal transition (EMT) markers.

CONCLUSION
GTF3A increases CSTA expression by binding to the *Csta* promoter, and increased CSTA level promotes CRC progression by regulating the EMT. Inhibition of GTF3A prevents CRC progression. Therefore, GTF3A is a potential novel therapeutic target and biomarker for CRC.

Key Words: Transcription factor IIIA; Cystatin A; Colorectal cancer; Epithelial-mesenchymal transition

Core Tip: Transcriptional factor III A (GTF3A) is highly expressed in colorectal cancer (CRC) tissues, and GTF3A expression is associated with CRC prognosis. GTF3A binds to the promoter of cystatin (*Csta*) gene to facilitate *Csta* transcription, which regulates the expression of epithelial-mesenchymal transition markers and promotes CRC progression. Blocking GTF3A significantly inhibits CRC cell growth. Therefore, GTF3A is a potential novel therapeutic target and prognostic biomarker for CRC.

INTRODUCTION

Colorectal cancer (CRC) is the third most commonly diagnosed cancer and the leading cause of cancer-related death worldwide[1]. CRC has distant invasive and metastatic abilities, such as liver and lung metastases, resulting in a poor survival[2]. Clarifying the molecular mechanisms underlying CRC progression is necessary for the development of new therapeutic strategies. Transcriptional factor III A (GTF3A), an RNA polymerase III transcriptional factor, specifically binds to the internal control region of the 5S rRNA gene from nucleotides +43 to +96[3], initiating the assembly of the transcription initiation complex (5S rDNA-TFIIIA-TFIIIC2-TFIIIBbeta complex). Complex formation is not proportional to the amount of TFIIIA[4]. GTF3A is present in all human organs. GTF3A shares a common conserved transcription activating signal, nuclear localization signal, and nuclear export signal, but lacks initiated Met and accompanying conserved residues in the N-terminal regions[5]. GTF3A regulates the 5S rRNA synthesis network by binding to 5S rDNA and 5S rRNA[6]. GTF3A binds to 5S rRNA to form the 7S ribonucleoprotein particle (RNP) complex, and the complex functions as a nuclear export signal (NES) to transfer 5S rRNA to the cytoplasm depending on the NES sequence, which protects the 5S rRNA from degradation[7,8]. Several studies have suggested that 5S rRNA binds to L5 and L11 to form the 5S RNP complex, regulating the MDM2-p53 checkpoint[9-12]. Alterations in ribosome biogenesis are critical drivers of tumorgenesis, and are closely associated with increased CRC cell growth[13]. These findings suggest that GTF3A regulates CRC progression.

Cystatin A (CSTA), a cysteine proteinase inhibitor, is a type 1 cystain (stefin). CSTA is a cornified cell envelope constituent of keratinocytes that plays a critical role in epidermal development and maintenance. The high expression of CSTA is associated with the invasion and metastasis of various malignant tumors, such as pancreatic ductal adenocarcinoma[14], esophageal squamous cell carcinoma [15], lung cancer[16], hepatocellular carcinoma (HCC)[17], and nasopharyngeal carcinoma (NPC)[18]. An increasing number of studies have shown that CSTA is a potential prognostic and diagnostic biomarker for cancer progression. The activity of the *Csta* promoter is positively regulated by the active Ras/MEKK1/MKK7/JNK signal transduction pathway, but negatively regulated by the negative Ras/Raf-1/MEK/ERK pathway in human keratinocytes[19]. Other cysteine protease inhibitors, cystatin SN (CST1) and cystatin S (CST4), are type 2 cystatin proteins, which enhance the metastasis of various malignant tumors and contribute to a poor patient survival[20,21]. CST1 overexpression increases cell migration and invasion by mediating the epithelial-mesenchymal transition (EMT) in breast cancer and HCC[22,23] and contributes to CRC cell proliferation[24]. CST1 is also considered an

early diagnostic biomarker and potential therapeutic target in breast cancer, CRC, and gastric cancer[25, 26]. In the present study, we showed that GTF3A was highly expressed in CRC, and it bound to the promoter of *Csta* to facilitate *Csta* transcription, which then regulated EMT marker expression and promoted CRC progression. Therefore, GTF3A is a potential novel therapeutic target and a prognostic biomarker for CRC.

MATERIALS AND METHODS

Reagents and antibodies
Dulbecco's modified Eagle's medium (DMEM), Cell Counting Kit (CCK8), and other supplements were obtained from Life Technologies (Rockville, MD, United States). GTF3A antibody for Western blot analysis was purchased from Bethyl Laboratories, Inc (Suzhou, China). CSTA antibody was purchased from Novus (CO, United States). CST1 antibody was purchased from Invitrogen (Shanghai, China). CST4 antibody was purchased from R&D Systems (Minneapolis, MN, United States). GTF3A antibody used for the immunofluorescence assay was purchased from Bioss Antibodies (Beijing, China). The dual-luciferase reporter assay system was purchased from Promega (Madison, WI, United States). Antibodies against Snail, E-cadherin, and beta-catenin were purchased from Abcam (Cambridge, United Kingdom). Glyceraldehydes-3-phosphate dehydrogenase (GAPDH) and secondary antibodies were purchased from Proteintech Company (Wuhan, Hubei, China).

Tissue microarray and immunohistochemical staining
Human tissue microarrays (HCol-Ade180Sur-08) containing 90 pairs of CRC tissues and adjacent non-tumor tissues, and human tissue microarrays (HCol-Ade060Lym-01) containing 20 pairs of CRC tissues, adjacent non-tumor tissues, and lymph node metastatic tissues, were purchased from Outdo Biotech Company (Shanghai, China). Immunohistochemical (IHC) staining was performed to detect the expression of GTF3A as described previously[27]. These tissue microarrays were stained with GTF3A antibody (1:300 dilution). The use of patient materials was approved by the ethics committee of Hunan Cancer Hospital (No. KYJJ-2020-004). All IHC results were evaluated based on the semi-quantitative histological scoring (HSCORE) system using the following formula: H-SCORE = $\sum$ (pi × i) ["pi" represents the percentage of stained cells in an intensity area, whereas "I" represents the staining intensity (0, no labeling; 1, weak; 2, moderate; and 3, strong)].

Cell lines
Human CRC cell lines (HCT116, SW480, DLD1, SW620, and HT29) were obtained from the American Type Culture Collection (Manassas, VA, United States) and were purchased from the Shanghai Cell Center (Shanghai, China). All cell lines were cultured in high-glucose DMEM supplemented with 10% fetal bovine serum (FBS) at 37 °C with 5% CO_2.

Real-time quantitative polymerase chain reaction
Real-time quantitative polymerase chain reaction (RT-qPCR) was performed as described previously [28]. Briefly, the total RNA of cultured cells was extracted using a total RNA kit (R6834, OMEGA), and 1 µg of DNase-treated RNA was reverse transcribed using the Revert Aid First Strand cDNA Synthesis Kit (Thermo Fisher Scientific, Shanghai, China) according to the manufacturer's instructions. The threshold cycle (Ct) values were measured using Hieff quantitative PCR SYBR Green Mix (Yeasen, Shanghai, China) in A LightCycler 96 qPCR System (Roche). Primer sequences used are listed in Supplementary Table 1. The relative mRNA levels of each gene were normalized to those of the housekeeping gene GAPDH. Relative transcript levels were calculated as two power values of $\triangle$ Ct (the differential value of Ct between GAPDH and the target cDNA).

Plasmid transfection
The designed short hairpin RNAs (shRNAs) shGTF3A#1, shGTF3A#2, shGTF3A#3, shGTF3A#4, and shscramble were cloned into the lentivirus vector GV112 by Shanghai GeneKai Company (Shanghai, China). The shRNA sequences for *Gtf3a* are listed in Supplementary Table 2. The shRNAs for the *Csta* gene were designed to knock down the expression of CSTA. The shRNA sequences for *Csta* are shown in Supplementary Table 3. Synthetic plasmids were verified by sequence analysis and PCR and then cloned into GV493. Lipofectamine 3000 (Thermo Fisher Scientific, Carlsbad, CA, United States) was used to transfect the plasmids into HEK293T cells; 1 × 10^5 cells were transfected with shscramble, shGTF3A#1, shGTF3A#2, shGTF3A#3, shGTF3A#4, shCSTA#1, and shCSTA#2. The knockdown efficiency was filtered using RT-qPCR.

Stable cell lines
shGTF3As, shCSTAs, and negative control lentiviruses were packaged by the Shanghai GeneKai Company (Shanghai, China). The lentivirus titers were quantified (≥ 10^8 TU/mL). Following the

manufacturer's protocol, 2×10^5 of SW480 and HCT116 cells were seeded in six-well culture plates, and cultivated at 37 °C and 5% CO$_2$. After 24 h, the cells were transfected with the appropriate amount of lentivirus at a multiplicity of infection of 20 TU/mL. After being incubated for 10 h, the culture medium was removed, and fresh DMEM containing 10% FBS was added. Next, antibiotic-free medium containing 3 μg/mL puromycin was used to screen the stable cells for 3-4 wk. Ultimately, the knockdown and negative control stable cell lines shscramble-SW480, shGTF3A#1-SW480, shGTF3A#4-SW480, shGTF3A#1-HCT116, and shGTF3A#4-HCT116 were obtained.

Western blot analysis
Western blotting was performed as previously described[29]. Briefly, 1×10^6 cells were lysed with a radioimmunoprecipitation assay lysis buffer [50 mmol/L Tris pH 7.4, 150 mmol/L NaCl, 1% Triton X-100, 1% sodium deoxycholate, and 0.1% sodium dodecyl sulfate (SDS)] containing 100 × protease inhibitor cocktail and 100 × phosphatase inhibitor cocktail (CWBIO, Beijing, China). Following the manufacturer's instructions, the crude lysate was centrifuged and the supernatant was collected to measure the protein concentration using the BCA Protein Assay Kit (CWBIO, Beijing, China). After being boiled at 100 °C for 5 min, 20-60 μg of protein was separated by 10% SDS- polyacrylamide gel electrophoresis and transferred to a 0.2 μm PVDF membrane (Millipore). The protein membrane was blocked with 5% non-fat milk, incubated with the primary antibody, and incubated with an appropriate peroxidase conjugated secondary antibody. The signal was detected on a gel imager using an enhanced chemiluminescence (ECL) Western blotting kit (CWBIO, Beijing, China). GAPDH was used as an internal control to verify basal expression. The ratio of specific proteins to GAPDH was calculated.

Cell proliferation and colony formation assays
shGTF3A#1-HCT116, shGTF3A#4-HCT116, shscramble-HCT116, shGTF3A#1-SW480, shGTF3A#4-SW480, and shscramble-SW480 cells were seeded in 96-well plates, and CCK8 (ApexBio) was used to examine cell viability following the manufacturer's protocol. Briefly, CCK8 was added to the cell plates, and incubated for 4 h. Then, the optical density at 450 nm was measured using a microplate reader. Cell viability was calculated daily for 5 d. For the colony formation assay, shGTF3A#1-HCT116, shGTF3A#4-HCT116, shscramble-HCT116, shGTF3A#1-SW480, shGTF3A#4-SW480, and shscramble-SW480 cells were seeded in 6-well plates with each well containing 1000 cells, and cultured for 16 d. The cell colonies were fixed in methanol, stained with 0.5% gentian violet, and counted automatically using a computerized microscope system.

Cell invasion and motility assays
Cell invasion and motility assays *in vitro* were performed using previously described methods[29]. Briefly, for the invasion assay, Matrigel (25 mg/50mL, Collaborative Biomedical Products, Bedford, MA, United States) was added to the upper chamber with 8 mm pore polycarbonate membrane filters. shGTF3A#1-HCT116, shGTF3A#4-HCT116, shscramble-HCT116, shGTF3A#1-SW480, shGTF3A#4-SW480, and shscramble-SW480 cells were seeded in the upper chamber (Neuro Probe, cabin John, MD) at a density of 1.5×10^4 cells/well in 100 μL of serum-free medium, and then incubated at 37 °C for 48 h. The bottom chamber contained standard medium with 20% FBS. Cells that invaded the lower surface of the membrane were fixed with 37% paraformaldehyde, and stained with crystal violet. Invading cells were counted under a light microscope. The motility assay was performed in a similar manner to the invasion assay without Matrigel coating.

Wound healing assay
A wound healing assay was used to measure the cell migration potential. Briefly, 2×10^5 of shGTF3A#1-HCT116, shGTF3A#4-HCT116, shscramble-HCT116, shGTF3A#1-SW480, shGTF3A#4-SW480, and shscramble-SW480 cells were seeded in 6-well plates. After the cells reached 95% confluence, the surface of the cell layer was wounded using a sterile 10 μL pipette tip. The cells were then rinsed three times with phosphate buffered saline (PBS) to move detached cells and incubated in DMEM containing 1% FBS for 48 h. Wound closure was observed under a microscope at 0, 24, and 48 h.

Tumor growth assay in vivo
In vivo tumor growth assays were performed as previously described[30]. Briefly, female nude mice (aged 4-5 wk) were obtained from Hunan SJA Laboratory Animal Co. Ltd. (Changsha, China). Experiments involving animal subjects and protocols for animal studies were approved by the Laboratory Animal Research Center of Hunan Cancer Hospital (No. 2020-118). Nude mice were subcutaneously injected with 3×10^6 shGTF3A#1-SW480, shGTF3A#4-SW480, or shscramble-SW480 cells (5 mice per group). The size of the tumor that developed in the mice was measured every 3 d, and a tumor growth curve was drawn. After 4 wk, the mice were euthanized with pentobarbital sodium at 20 mg/mI, and the tumor weights were measured.

RNA sequencing and data analysis

After harvesting shGTF3A#1-SW480, shGTF3A#4-SW480, and shscramble-SW480 cells, total RNA was extracted using TRIzol reagent (Invitrogen). After the rRNA was removed, the enriched longRNA (> 200 nt) was interrupted, reversely transcribed into cDNA, and repaired, and RNA sequencing (RNA-Seq) was performed to build a chain-specific database. The clean data were obtained by quality testing of Bioptic Qsep100, and then comparative mapping of genomes was acquired between clean data and the hg38 Ensemble transcriptome using HISAT2 software. The differentially expressed genes between groups were analyzed using the DESeq2 R package, and the default screening criteria were: (1) Log2 (fold change) >1; and (2) False discovery rate < 0.05.

Fluorescence in situ hybridization assay

Fluorescence *in situ* hybridization (FISH) assays were performed as previously described[31]. FISH probes for *Csta* promoter sequence were designed and synthesized by Well Bio (Guangzhou, China). The lncRNA FISH kit (C10910) was purchased from Wellbio (Guangzhou, China). The cell slides were fixed with 4% paraformaldehyde for 30 min at 25 °C, permeabilized with proteinase K for 30 min at 37 °C, and blocked for 30 min at 37 °C with 200 µL of pre-hybridization solution. After removing the pre-hybridization solution, 100 µL of the probe hybridization solution was added to the cell slides overnight at 37 °C in the dark. After being washed three times for 5 min each with 4 × SSC, 2 × SSC, 1 × SSC, and PBS, the cell slides were incubated with the appropriately diluted primary antibody (anti-GTF3A) overnight at 4 °C. After washing three times with PBS, the slides were incubated with the secondary antibody (fluorescence labelled anti-rabbit immunoglobulin G) for 90 min at 37 °C. Finally, the slides were stained with 4',6-diamidino-2-phenylidole for 10 min at 37 °C and sealed with 90% glycerin. All images were acquired using a fluorescence microscope.

Electrophoretic mobility shift assay

A biotin labeled *Csta* promoter DNA probe (5'-biotin-agctagtgacgcctttttaaaacacgt ccaccattccttccttttttc-3') was synthesized by Sangon (Shanghai, China). Both sense and antisense strands were diluted to a concentration of 0.2 µM, mixed at 1:1, denatured at 95 °C for 5 min, maintained at 70 °C for 20 min, and formed into a double-stranded probe (diluted 10 times when used) after being cooled to room temperature. Following the instructions of the electrophoretic mobility shift assay (EMSA) kit (CWBIO, Beijing, China), the protein supernatant for each sample was separated on a 4% polyacrylamide gel, and transferred to a nylon membrane (CWBIO). The protein membrane was cross-linked using UV radiation, blocked with a confining liquid, and incubated with the indicated streptavidin-horseradish peroxidase conjugate. The signal was detected on a gel imager using the ECL Western blotting kit (CWBIO, Beijing, China).

Luciferase activity assay

A dual-luciferase reporter assay system (Promega) was used to detect the expression of *Csta* following the manufacturer's instructions. Briefly, the *Csta* promoter was cloned into the firefly luciferase plasmid, and *Csta* promoter-luc was obtained. Then, 1 × 10⁵ of HCT116 cells were cultured in 48-well plates. *Csta* promoter-luc, plasmid-Renilla, and plasmid-GTF3A were co-transfected into HCT116 cells with X-tremeGene HP. After 48 h of culture, the cells were harvested, lysed with Passive Lysis Buffer, and treated with Luciferase Assay Reagent. Firefly luciferase and renilla luciferase were measured. The ratio of firefly luciferase to renilla luciferase represents the expression of *Csta*.

Statistical analysis

All experiments were performed at least three times. The results are presented as the mean ± SD of three independent experiments and were analyzed using Student's *t*-test. The differences between groups are reported as follows: [a]P < 0.05, [b]P < 0.01, [c]P < 0.001, and P > 0.05. All statistical data were calculated using GraphPad Prism software (version7.0).

RESULTS

High expression of GTF3A in CRC and metastatic tissues

To determine the expression of GTF3A in CRC tissues, two sets of CRC tissue microarray were used to detect GTF3A expression by IHC. GTF3A was found to have higher expression in the cancer tissues than in the adjacent tissues of HCol-Ade180Sur-08 microarray. To further probe whether metastatic cancers had higher expression and analyze the association of GTF3A expression with metastasis, HCol-Ade060Lym-01 microarray containing CRC cancer, metastatic tissues, and adjacent tissues was also used to detect GTF3A, and observe GTF3A expression in metastatic tissues. These two microarrays had a total of 110 cancer tissues, 110 adjacent tissues, and 20 metastatic tissues, some of which were chipped off and could not be used; 102 cases in the cancer group, 106 in the adjacent group, and 20 in the metastatic group were calculated by gray scanning and scored, and survival time and survival curve
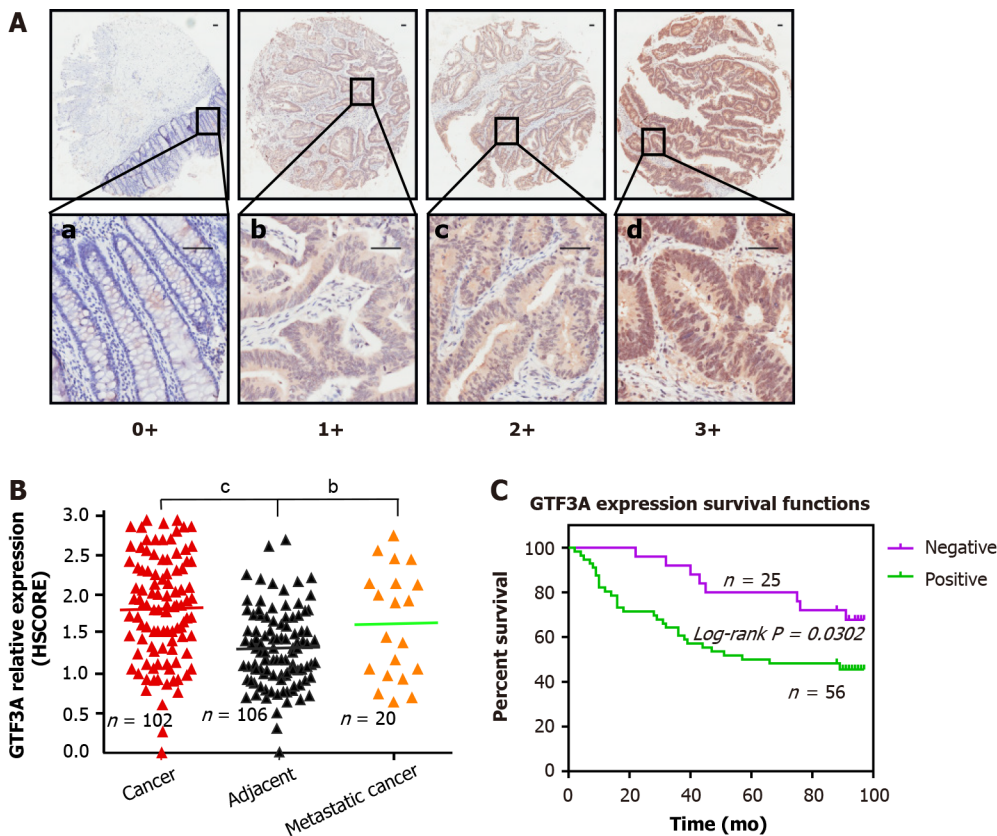
Figure 1 Transcriptional factor III A expression in colorectal cancer and survival analysis of patients with colorectal cancer. A: Transcriptional factor III A (GTF3A) expression in adjacent normal, colorectal cancer (CRC), and metastatic tissues were detected using immunohistochemical staining. The grading standards were: (1) Negative, a, scored as 0; (2) Weakly positive, b, scored as 1; (3) Moderately positive, c, scored as 2; and (4) Strongly positive, d, scored as 3. Scale bar, 50 μm; B: GTF3A expression in adjacent normal, CRC, and metastatic tissues was quantified using semi-quantitative histological score. Scored dots expression groups were statistically analyzed using unpaired *t* test; C: Overall survival of patients with GTF3A negative (*n* = 25) or GTF3A positive (*n* = 56) expression was analyzed by log-rank (Mantel-Cox) test. [b]P < 0.01; [c]P < 0.001. GTF3A: Transcriptional factor III A; HSCORE: Semi-quantitative histological score.

were analyzed. The expression of GTF3A in CRC and metastatic tissues was higher than that in adjacent normal tissues (Figures 1A and B, P < 0.01). To analyze whether GTF3A expression was relevant to survival time, patients with CRC were divided into GTF3A negative and positive groups, and the survival curve of CRC patients showed that the negative group had a longer overall survival than the positive group (Figure 1C, P < 0.05). These clinical data suggested that GTF3A expression is associated with CRC progression.

Knockdown of the *Gtf3a* gene inhibits CRC cell proliferation

Five CRC cell lines, HCT116, SW480, DLD1, SW620, and HT-29, were used to detect the expression of GTF3A using Western blot. The results showed that SW480 cells had high expression of GTF3A, whereas HCT116, DLD1, SW620, and HT-29 cells had low expression of GTF3A (Figure 2A). To clarify the role of *Gtf3a* in CRC, shGTF3A#1, #2, #3, and #4 were designed and packaged into the virus. Their inhibitory effects on *Gtf3a* were screened, and the results showed that shGTF3A#1 and shGTF3A#4 had high knockdown efficiencies. HCT116 and SW480 cells were stably transfected with shscramble, shGTF3A#1, or shGTF3A#4. RT-qPCR was performed to evaluate knockdown efficiency, and the results showed that shGTF3A#1 and shGTF3A#4 induced effective knockdown of *Gtf3a* in HCT116 and SW480 cells (Figure 2B). Consistently, Western blot results showed that GTF3A protein expression was effectively decreased in shGTF3A#1 and #4-HCT116 and shGTF3A#1 and #4-SW480 cells (Figure 2B). The cell viability of HCT116 and SW480 cells was detected using the CCK8 assay after knockdown of the *Gtf3a* gene, and the cell proliferation of HCT116 and SW480 cells was significantly decreased in the knockdown group (Figure 2B). Furthermore, the cell colony formation assay showed that colony size and number were dramatically diminished in *Gtf3a*-knockdown cells (Figure 2C, P < 0.01). These data indicated that knockdown of *Gtf3a* inhibits the growth of CRC cells.

Knockdown of *Gtf3a* inhibits CRC cell motility and invasion

Gtf3a-knockdown SW480 and HCT116 cells were used to determine whether *Gtf3a* is involved in CRC cell motility and invasion. Results of the wound healing assay showed that shGTF3A#1 and #4-HCT116
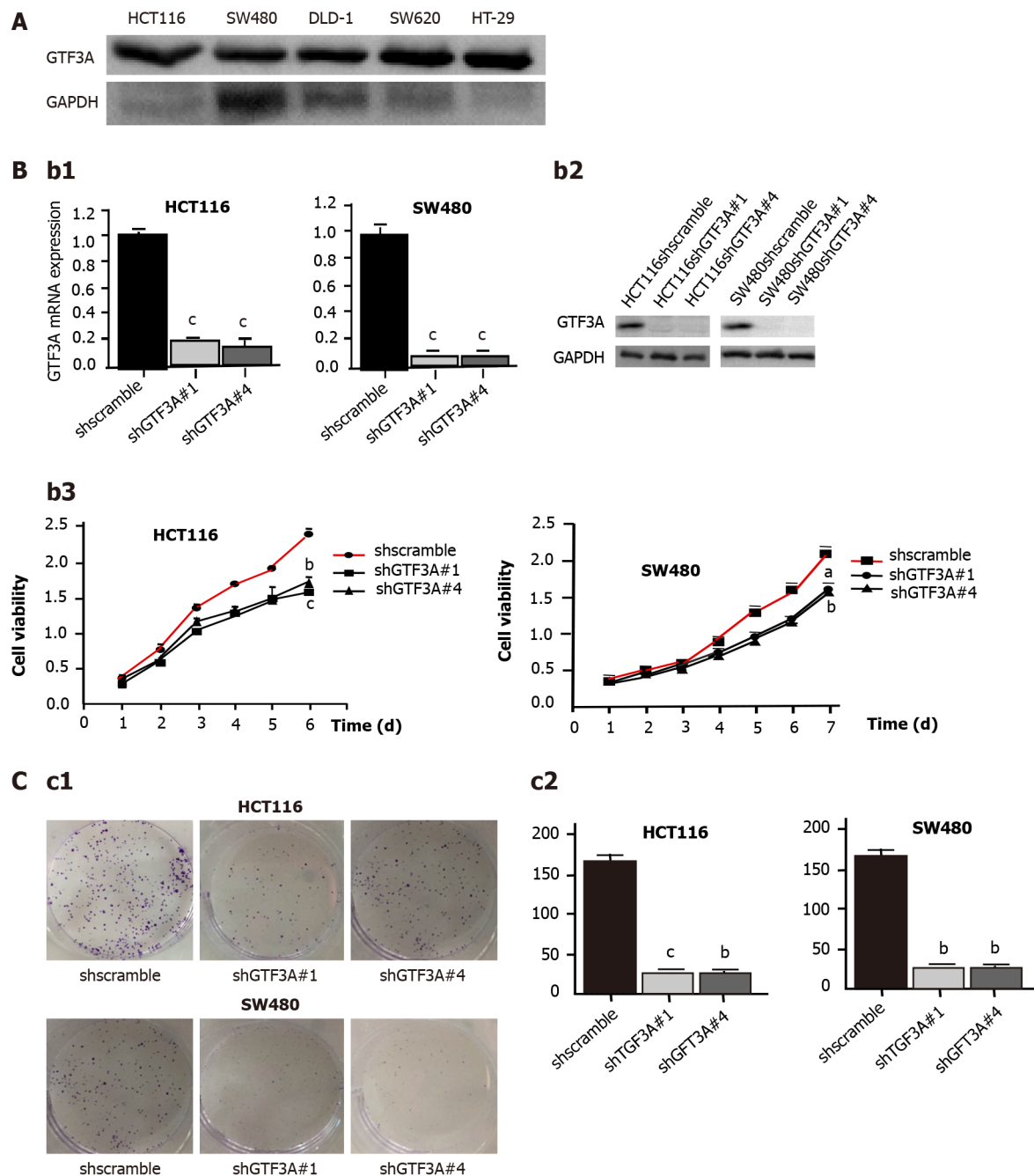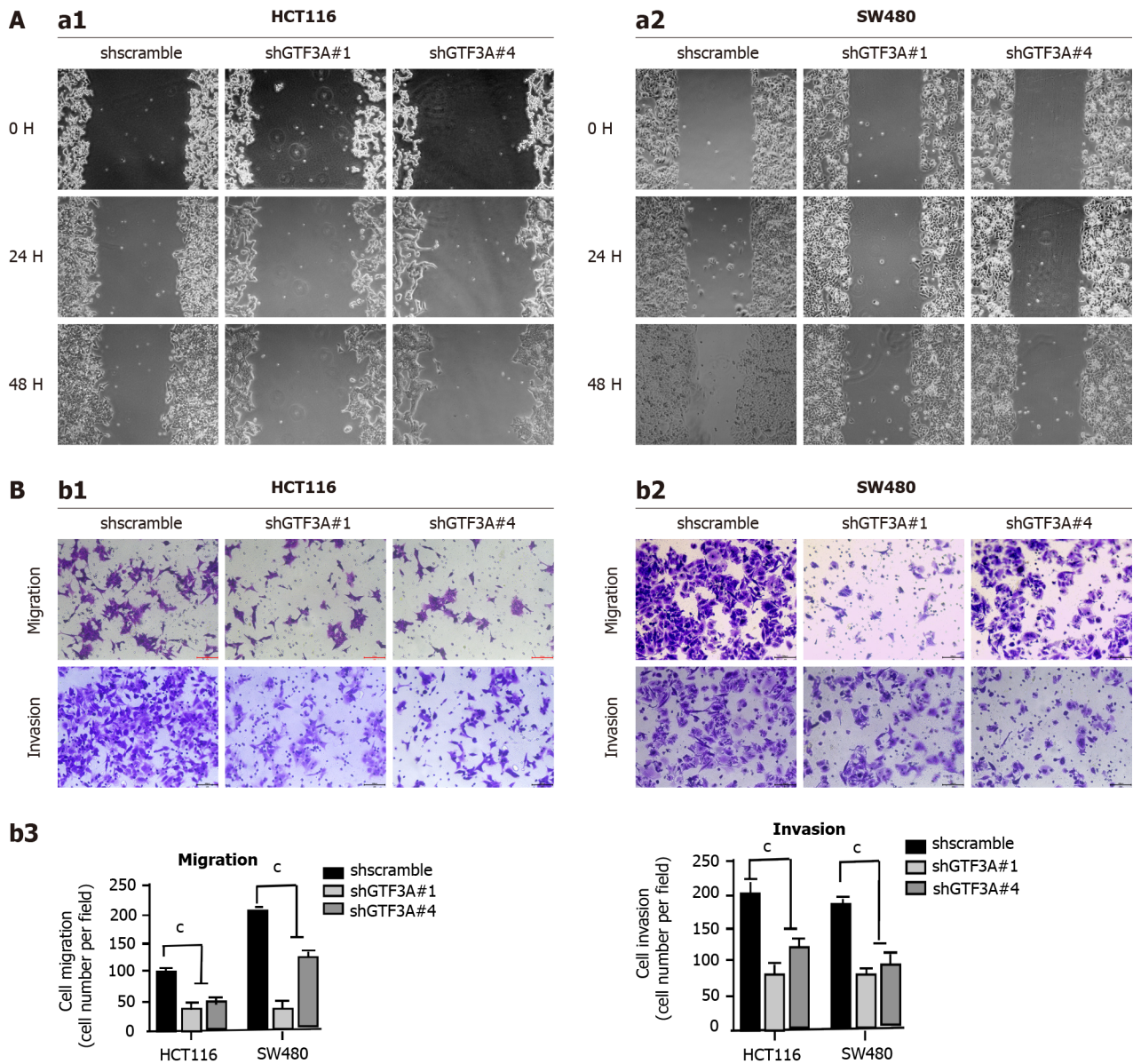
Figure 2 Knockdown of transcriptional factor III A gene inhibits colorectal cancer cell proliferation. A: The expression of transcriptional factor III A (GTF3A) in HCT116, SW480, DLD-1, SW620, and HT-29 cells was detected by Western blot; B: HCT116 and SW480 cells were stably transfected with short hairpin (sh) shscramble and shGTF3A#1 and #4-GV112 virus, respectively. *Gtf3a* mRNA (b1) and GTF3A protein (b2) expression were detected using real-time quantitative polymerase chain reaction and Western blot, respectively. The cell viability of HCT116 and SW480-shscramble as well as shGTF3A#1 and #4 cells was detected using Cell Counting Kit assay (b3); C: Colony formation of the transfected HCT116 and SW480 cells was detected using colony formation assay (c1), and the colony number was counted (c2). *Gtf3a* mRNA expression, cell colony number, and cell viability are expressed as the mean ± SEM of three independent experiments. [a]$P < 0.05$; [b]$P < 0.01$; [c]$P < 0.001$. GTF3A: Transcriptional factor III A; GAPDH: Glyceraldehydes-3-phosphate dehydrogenase.

and shGTF3A#1 and #4-SW480 cells had impaired migratory capability compared with shscramble cells (Figure 3A). In addition, the transwell assay showed that invasion and metastasis in the *Gtf3a*-knockdown groups were significantly repressed compared with those in the controls (Figure 3B), and the number of invaded or migrated cells in the knockdown groups dramatically decreased (Figure 3B). Collectively, these results highlighted that knockdown of *Gtf3a* suppressed CRC cell invasion and metastasis in *vitro*, whereas the *Gtf3a* gene promoted the progression of CRC.

GTF3A protein regulates CSTA by binding to the CSTA promoter

To explore the molecular mechanisms of GTF3A in CRC progression, RNA-Seq was used to screen the target genes of GTF3A, and the differential genes between SW480 *Gtf3a*-knockdown and scramble control cells were analyzed. The RNA-Seq results are shown in Figures 4A and 4B; several differentially
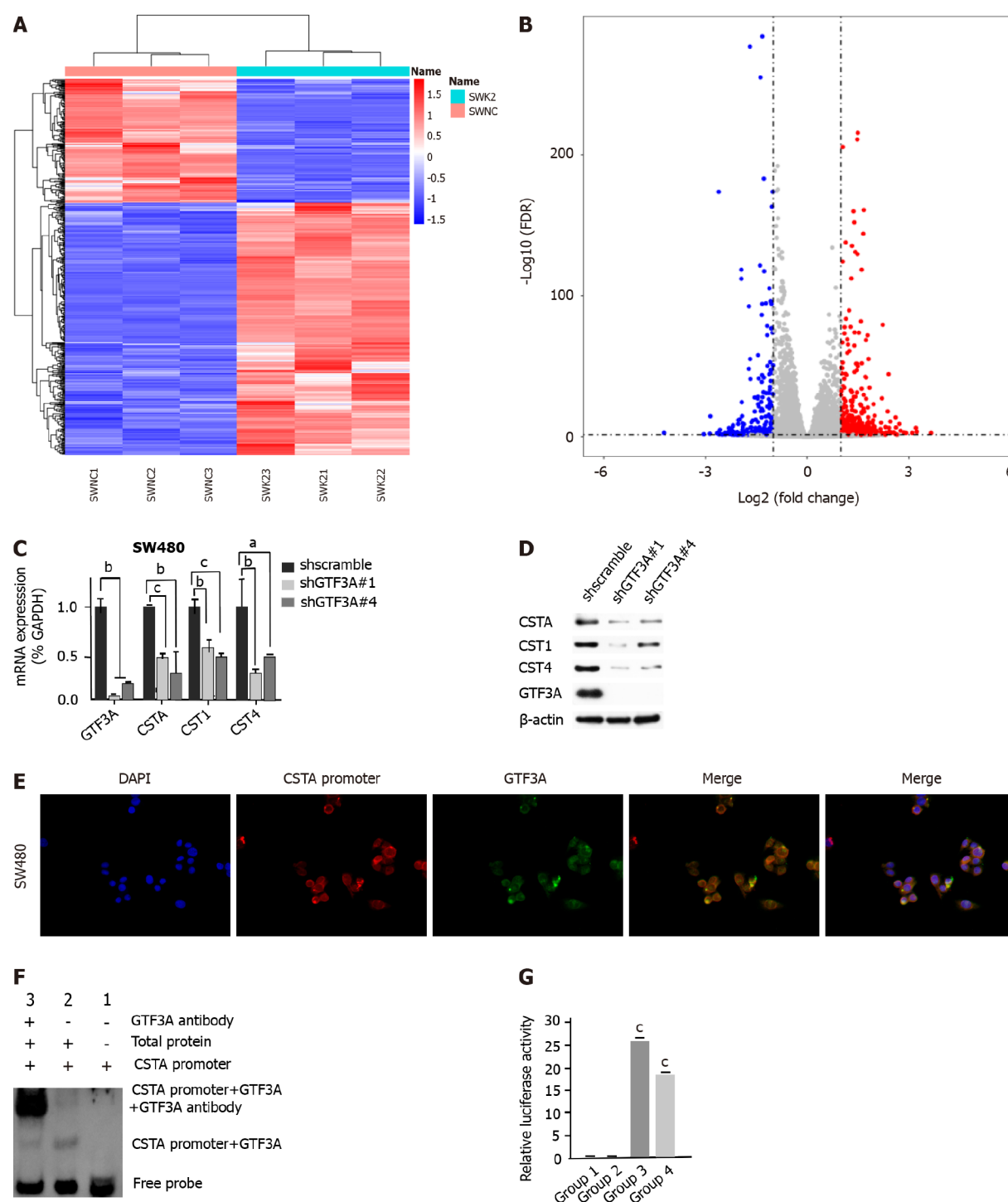
Figure 3 Knockdown of transcriptional factor III A gene inhibits the invasion and migration of colorectal cancer cell *in vitro*. A: The migratory abilities of short hairpin (sh) GTF3A#1 and #4-HCT116 cells were detected using wound-healing assay (a1). The migratory abilities of shGTF3A#1 and #4-SW480 cells were detected as above (a2); B: The migratory and invasive capabilities of shGTF3A#1 and #4-HCT116 (b1) and shGTF3A#1 and #4-SW480 cells (b2) were detected using transwell assay. The migrated and invaded cells were counted (b3). Migratory and invasive capabilities are expressed as the mean ± SEM of three independent experiments. $^{c}P < 0.001$.

expressed genes were found between the groups (Figures 4A and 4B, Supplementary Table 4). In particular, the expression of *Csta*/*Cst1*/*Cst4* genes in *Gtf3a*-knockdown cells was dramatically lower than that in the control group (Supplementary Table 4). *Csta*/*Cst1*/*Cst4* genes, members of the cystatin superfamily that encode cysteine protease inhibitors, are overexpressed in various types of cancers, subsequently promoting cancer cell metastasis and resulting in a poor prognosis[14-16]. RT-qPCR and Western blot results showed that the expression of *Csta*/*Cst1*/*Cst4* genes was significantly decreased in *Gtf3a*-knockdown cells (Figures 4C and 4D).

The results of the RNA-Seq showed that CSTA had the largest difference after knockdown of *Gtf3a* in FISH experiments; the sequence probe of the *Csta* promoter was labeled with red fluorescence, whereas GTF3A was labeled with green fluorescence. The fluorescence staining of the GTF3A and *Csta* promoters was colocalized to a large extent as indicated by an orange-yellow fused fluorescence (Figure 4E), suggesting that GTF3A binds with the *Csta* promoter. To confirm the interaction between GTF3A and the *Csta* promoter, EMSA was performed to directly observe the interaction of GTF3A and the *Csta* promoter. The results showed that GTF3A interacted with the *Csta* promoter (Figure 4F). Next, a dual-luciferase assay was carried out to determine whether the interaction of GTF3A with *Csta* promoter increased *Csta* expression, and the results showed that the transcript activity of the *Csta* gene was significantly increased after transfection with CSTA (Figure 4G, $P < 0.05$). These data suggested that GTF3A binds to the *Csta* promoter to regulate its transcription and translation.
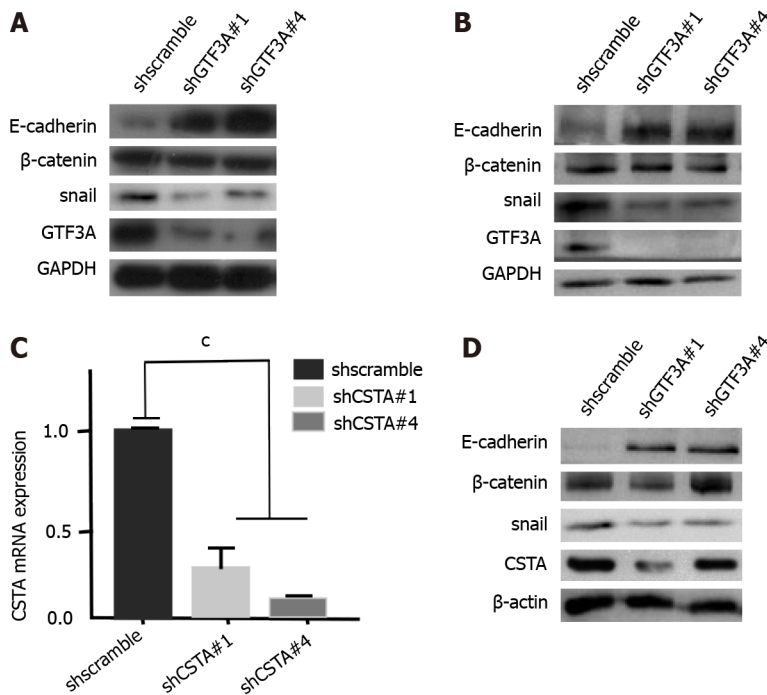
Figure 4 Transcriptional factor III A regulates cystatin A by binding to the promoter of cystatin A gene. A: Heat map of RNA-sequencing (RNA-Seq) for transcriptional factor III A *gene (Gtf3a)*-knockdown and scramble control cells; B: Volcano plot of RNA-Seq for *Gtf3a*-knockdown and scramble control cells; C: mRNA expression of *Gtf3a*, cystatin A (*Csta*), cystatin SN gene (*Cst1*), and cystatin S genes (*Cst4*) in short hairpin (sh)scramble-SW480 and shGTF3A#1 and #4-SW480 cells were detected using real-time quantitative polymerase chain reaction; D: GTF3A, CSTA, CST1, and CST4 in shscramble-SW480 and shGTF3A#1 and #4-SW480 cells were detected using Western blot; E: RNA fluorescence *in situ* hybridization was performed to verify the locations of the *Csta* promoter probe (lncRNA) and GTF3A in SW480 cells; F: Electrophoretic mobility shift assay (EMSA) was used to test the interaction of the *Csta* promoter and GTF3A. The *Csta* promoter plus GTF3A antibody as the super shift in EMSA; G: Luciferase activity assay was used to detect the interaction of GTF3A with the *Csta* promoter and the transcription of *Csta*. Group 1 (*Csta* promoter-luc blank vector plus GTF3A blank plasmid) and group 2 (*Csta* promoter-luc blank vector plus GTF3A-plasmid) served as the control groups, and group 3 (*Csta* promoter-luc plus GTF3A) and group 4 (*Csta* promoter-luc plus GTF3A blank vector) as experimental groups. *Csta* expression is expressed as the mean ± SEM of three independent experiments. $^cP < 0.001$. GTF3A: Transcriptional factor III A; GAPDH: Glyceraldehydes-3-phosphate dehydrogenase; CSTA: Cystatin A; CST1: Cystatin SN; CST4: Cystatin S.

GTF3A mediates CRC cell EMT by regulating the expression of CSTA

The above results indicated that GTF3A promoted CRC cell invasion and metastasis. To investigate the underlying mechanisms, EMT markers, such as Snail, E-cadherin, and beta-catenin, were detected in

Figure 5 Transcriptional factor III A mediates epithelial-mesenchymal transition of colorectal cancer cells by regulating cystatin A. A: Epithelial-mesenchymal transition (EMT) biomarkers E-cadherin, beta-catenin, and snail in short hairpin of transcriptional factor III A (shGTF3A) #1 and #4-HCT116 cells and the control group were detected by Western blot; B: EMT biomarkers were tested in shGTF3A#1 and #4-SW480 cells and the control group; C: mRNA expression of cystatin A (*Csta*) gene in shCSTA#1,2-SW480 and the control group was detected using real-time quantitative polymerase chain reaction; D: EMT biomarkers were analyzed in *Csta*-knockdown SW480 and the control cells. Cystatin A mRNA expression is expressed as the mean ± SEM of three independent experiments. There were statistically significant differences between shCSTA#1,2-SW480 and the control group. $^c P < 0.001$. GTF3A: Transcriptional factor III A; GAPDH: Glyceraldehydes-3-phosphate dehydrogenase; CSTA: Cystatin A; shscramble: Short hairpin scramble; shCSTA: Short hairpin of transcriptional factor III A.

scrambled control and *Gtf3a*-knockdown cells. Western blot results showed that *Gtf3a*-knockdown HCT116 and SW480 cells had decreased Snail expression and increased E-cadherin expression compared with the scrambled control (Figures 5A and 5B). Moreover, GTF3A regulates the expression of CSTA/CST1/CST4, and CST1 promotes the migration and invasion of breast cancer cells by up-regulating E-cadherin[23]. Consistent with these results, *Csta*-knockdown cells were constructed (Figure 5C), and Snail, E-cadherin, and beta-catenin were detected in these cells. The cells showed down-regulated Snail expression and upregulated E-cadherin expression (Figure 5D). Collectively, GTF3A may mediate the EMT to promote CRC cell metastasis by regulating CSTA and CST1 expression.

GTF3A promotes CRC cell growth in vivo

The above results showed that GTF3A promoted the proliferation, invasion, and metastasis of CRC cells *in vitro*. To verify whether GTF3A promotes CRC progression *in vivo*, nude mice were subcutaneously injected with the *Gtf3a*-knockdown and control cells to examine the function of *Gtf3a*. After 28 d, the *Gtf3a*-knockdown group had a significantly smaller tumor size (Figures 6A and 6B) and slower tumor growth (Figure 6C, $P < 0.05$) than the control group. In addition, the *Gtf3a*-knockdown group showed a reduction in tumor weights (Figure 6D, $P < 0.05$). *In vivo* experiments demonstrated that GTF3A promoted the growth of CRC cells.

DISCUSSION

As a transcription factor of RNA polymerase III, GTF3A is homologous to TFIIIB and TFIIIC, which guides the accurate transcription of 5S RNA genes[32]. RNA polymerase III is responsible for the transcription of non-coding genes including U6 snRNA, tRNA, and 5S RNA[33]. Deregulation of RNA polymerase III leads to the development of a large variety of human disorders[34], and upregulation of RNA polymerase III transcription has been observed in various types of cancer[35,36]. TFIIIB and TFIIIC can enhance the transcriptional activity of RNA polymerase III and mediate cellular transformation and tumor formation[37-40]. In addition, TFIIIA-mediated 5S rRNA is an essential component of 5S RNP that regulates the Hdm^2-p53 checkpoint to affect ribosome biosynthesis and cancer progression[9-13], indicating that GTF3A participates in the occurrence and development of various cancer types. Overex-pression of GTF3A has been observed in CRC tumors and metastatic tissues using CRC tissue arrays, and clinical data analysis suggests that GTF3A is associated with CRC progression and metastasis.
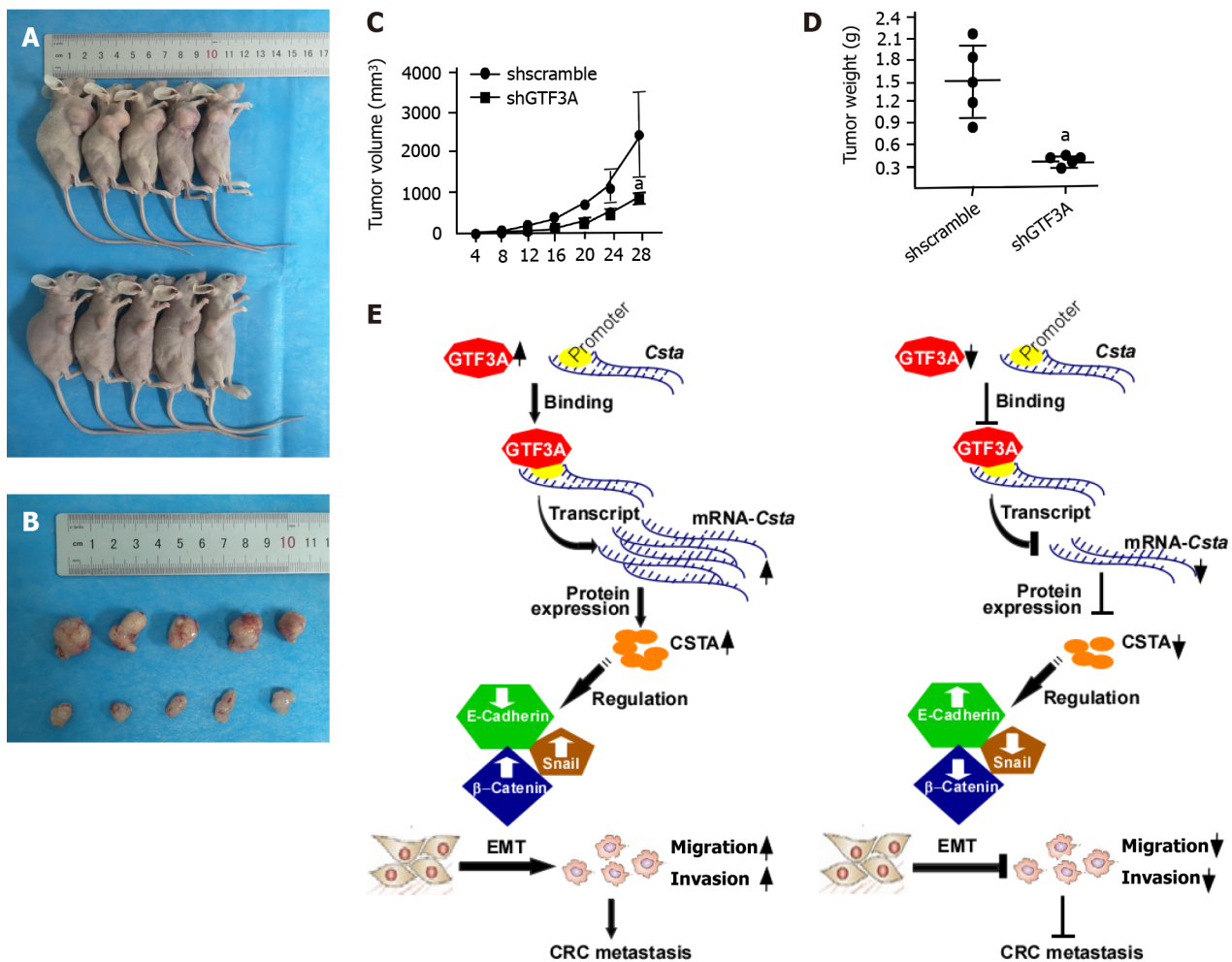
Figure 6 Transcriptional factor III A promotes colorectal cancer growth *in vivo*. A: Short hairpin of transcriptional factor III A (shGTF3A)-HCT116 and short hairpin of scramble (shscramble)-HCT116 cells were subcutaneously injected into the right armpit of nude mice. After 28 d, the mice were euthanized, and the images of the representative nude mice are shown; B: Tumors were stripped from the nude mouse; C: The tumor growth curve of shGTF3A-HCT116 and shscramble-HCT116 cells was calculated by tumor volume; D: The removed tumors of shGTF3A-HCT116 and shscramble-HCT116 cells were weighed; E: Schematic diagram of GTF3A-promoting CRC metastasis. GTF3A bound to the promoter of cystatin A (*Csta*) gene to increase *Csta* gene transcription and protein expression, increased CSTA regulated the epithelial-mesenchymal transition (EMT) to promote invasion and metastasis of colorectal cancer (CRC) cells, while knockdown of *Gtf3a* decreased CSTA expression, inhibited the EMT, and reduced CRC cell invasion and metastasis. [a]$P < 0.05$. shscramble: Short hairpin scramble; shCSTA: Short hairpin of transcriptional factor III A; EMT: Epithelial-mesenchymal transition; CRC: Colorectal cancer; CSTA: Cystatin A.

A series of *in vitro* and *in vivo* experiments was performed to examine the role of GTF3A in CRC development. The results showed that the knockdown of *Gtf3a* inhibited the proliferation, invasion, and metastasis of CRC cells. Generally, cancer metastasis is mostly related to the EMT[41]. We hypothesized that GTF3A promotes CRC cell metastasis by mediating the EMT. Thus, the EMT biomarkers Snail, vimentin, beta-catenin, and E-cadherin were detected. These changes in Snail and E-cadherin levels were in accordance with our hypothesis. The vimentin had no changed after knockdown of GTF3A (not shown). Both RNA-Seq and RT-qPCR showed that *Csta* expression was dramatically decreased in *Gtf3a*-knockdown cells. Furthermore, the luciferase activity assay suggested that GTF3A regulates the *Csta* transcription and translation by binding to the *Csta* promoter, therefore, *Csta* is a target gene of GTF3A.

CSTA is associated with invasion and metastasis in various cancer types[17,19,22], and *in vitro* experiments have shown that CSTA modulates the invasion and metastasis of NPC cells[18]. Based on our data, GTF3A may regulate *Csta* expression to mediate the EMT and promote CRC metastasis. FISH and EMSA results suggested that GTF3A binds with the promoter of the *Csta* gene, and the luciferase activity assay showed that GTF3A upregulated *Csta* transcription by binding to the *Csta* promoter. In addition, CSTA regulates E-cadherin and Snail expression, there mediating the EMT shift. Collectively, GTF3A upregulates CSTA expression to promote CRC metastasis by accelerating EMT shift. CST1 is associated with the progression and prognosis of various cancer types[20,25], and its overexpression modulates EMT progression by modulating the PI3K/AKT pathway *in vivo* and *in vitro*[22].

CONCLUSION

GTF3A increases *Csta* gene transcription and protein expression by binding to the *Csta* promoter, increases the expression of CSTA, enhances the EMT process, and facilitates CRC cell invasion and metastasis. However, knockdown of *Gtf3a* decreases CSTA expression, inhibits the EMT, and suppresses CRC cell invasion and metastasis (Figure 6E). Therefore, GTF3A is a potential novel therapeutic target and prognostic biomarker in human CRC.

ARTICLE HIGHLIGHTS

Research background

Advanced colorectal cancer (CRC) generally has poor outcomes and high mortality rates. Clarifying the molecular mechanisms underlying CRC progression is necessary to develop new diagnostic and therapeutic strategies to improve CRC outcome and decrease mortality.

Research motivation

Transcriptional factor III A (GTF3A), an RNA polymerase III transcriptional factor, is a critical driver of tumorgenesis and aggravates CRC cell growth. The mechanism of GTF3A participating in CRC is not clear.

Research objectives

To confirm whether GTF3A aggravates CRC progression and investigate molecular mechanisms underlying CRC progression.

Research methods

Immunohistochemistry was used to detect GTF3A expression in CRC tissues. Short hairpin GTF3As and CSTAs were designed and packaged into the virus to block the expression of *Gtf3a* and *Csta* genes. RNA sequencing and data analysis was used to screen the target genes of GTF3A. Fluorescence *in situ* hybridization assay was used to detect the interaction of GTF3A with *Csta*, and luciferase activity assay was used to evaluate the expression of *Gtf3a* and *Csta* genes.

Research results

GTF3A was highly expressed in CRC tissues and metastatic tissues, and its expression was associated with CRC prognosis. Knockdown of the *Gtf3a* gene impaired CRC cell proliferation, invasion, and motility *in vitro* and *in vivo*. GTF3A increased *Csta* transcription, and increased CSTA upregulated epithelial-mesenchymal transition (EMT) markers.

Research conclusions

GTF3A increases CSTA expression by binding to the *Csta* promoter, and increased CSTA levels promote CRC progression by regulating EMT. Inhibition of GTF3A prevents CRC progression.

Research perspectives

GTF3A may be a potential novel therapeutic target and biomarker for CRC.

ACKNOWLEDGEMENTS

FOOTNOTES

Institutional animal care and use committee statement: All procedures involving animals were reviewed and approved by the Institutional Animal Care and Use Committee of the Hunan Cancer Hospital (No. 2020-118).

Conflict-of-interest statement: All the authors report no relevant conflicts of interest for this article.

Data sharing statement: No additional data are available.

ARRIVE guidelines statement: The authors have read the ARRIVE Guidelines, and the manuscript was prepared and revised according to the ARRIVE Guidelines.

Open-Access: This article is an open-access article that was selected by an in-house editor and fully peer-reviewed by external reviewers. It is distributed in accordance with the Creative Commons Attribution NonCommercial (CC BY-NC 4.0) license, which permits others to distribute, remix, adapt, build upon this work non-commercially, and license their derivative works on different terms, provided the original work is properly cited and the use is non-commercial. See: https://creativecommons.org/Licenses/by-nc/4.0/

Country/Territory of origin: China

ORCID number: Jing Wang 0000-0002-6594-3494; Yuan Tan 0000-0003-0362-4073; Qun-Ying Jia 0000-0003-4660-3790; Fa-Qin Tang 0000-0001-5794-4975.

S-Editor: Wang JJ
L-Editor: Wang TQ
P-Editor: Yuan YY

REFERENCES

1   **Jemal A**, Bray F, Center MM, Ferlay J, Ward E, Forman D. Global cancer statistics. *CA Cancer J Clin* 2011; **61**: 69-90 [PMID: 21296855 DOI: 10.3322/caac.20107]

2   **Riihimäki M**, Hemminki A, Sundquist J, Hemminki K. Patterns of metastasis in colon and rectal cancer. *Sci Rep* 2016; **6**: 29765 [PMID: 27416752 DOI: 10.1038/srep29765]

3   **Seifart KH**, Wang L, Waldschmidt R, Jahn D, Wingender E. Purification of human transcription factor IIIA and its interaction with a chemically synthesized gene encoding human 5 S rRNA. *J Biol Chem* 1989; **264**: 1702-1709 [PMID: 2912980]

4   **Weser S**, Riemann J, Seifart KH, Meissner W. Assembly and isolation of intermediate steps of transcription complexes formed on the human 5S rRNA gene. *Nucleic Acids Res* 2003; **31**: 2408-2416 [PMID: 12711686 DOI: 10.1093/nar/gkg345]

5   **Hanas JS**, Hocker JR, Cheng YG, Lerner MR, Brackett DJ, Lightfoot SA, Hanas RJ, Madhusudhan KT, Moreland RJ. cDNA cloning, DNA binding, and evolution of mammalian transcription factor IIIA. *Gene* 2002; **282**: 43-52 [PMID: 11814676 DOI: 10.1016/s0378-1119(01)00796-x]

6   **Schulman DB**, Setzer DR. Identification and characterization of transcription factor IIIA from Schizosaccharomyces pombe. *Nucleic Acids Res* 2002; **30**: 2772-2781 [PMID: 12087160 DOI: 10.1093/nar/gkf385]

7   **Fridell RA**, Fischer U, Lührmann R, Meyer BE, Meinkoth JL, Malim MH, Cullen BR. Amphibian transcription factor IIIA proteins contain a sequence element functionally equivalent to the nuclear export signal of human immunodeficiency virus type 1 Rev. *Proc Natl Acad Sci U S A* 1996; **93**: 2936-2940 [PMID: 8610146 DOI: 10.1073/pnas.93.7.2936]

8   **Layat E**, Probst AV, Tourmente S. Structure, function and regulation of Transcription Factor IIIA: From Xenopus to Arabidopsis. *Biochim Biophys Acta* 2013; **1829**: 274-282 [PMID: 23142779 DOI: 10.1016/j.bbagrm.2012.10.013]

9   **Sloan KE**, Bohnsack MT, Watkins NJ. The 5S RNP couples p53 homeostasis to ribosome biogenesis and nucleolar stress. *Cell Rep* 2013; **5**: 237-247 [PMID: 24120868 DOI: 10.1016/j.celrep.2013.08.049]

10   **Donati G**, Peddigari S, Mercer CA, Thomas G. 5S ribosomal RNA is an essential component of a nascent ribosomal precursor complex that regulates the Hdm2-p53 checkpoint. *Cell Rep* 2013; **4**: 87-98 [PMID: 23831031 DOI: 10.1016/j.celrep.2013.05.045]

11   **Onofrillo C**, Galbiati A, Montanaro L, Derenzini M. The pre-existing population of 5S rRNA effects p53 stabilization during ribosome biogenesis inhibition. *Oncotarget* 2017; **8**: 4257-4267 [PMID: 28032591 DOI: 10.18632/oncotarget.13833]

12   **Nishimura K**, Kumazawa T, Kuroda T, Katagiri N, Tsuchiya M, Goto N, Furumai R, Murayama A, Yanagisawa J, Kimura K. Perturbation of ribosome biogenesis drives cells into senescence through 5S RNP-mediated p53 activation. *Cell Rep* 2015; **10**: 1310-1323 [PMID: 25732822 DOI: 10.1016/j.celrep.2015.01.055]

13   **Nait Slimane S**, Marcel V, Fenouil T, Catez F, Saurin JC, Bouvet P, Diaz JJ, Mertani HC. Ribosome Biogenesis Alterations in Colorectal Cancer. *Cells* 2020; **9** [PMID: 33120992 DOI: 10.3390/cells9112361]

14   **Komura T**, Takabatake H, Harada K, Yamato M, Miyazawa M, Yoshida K, Honda M, Wada T, Kitagawa H, Ohta T, Kaneko S, Sakai Y. Clinical features of cystatin A expression in patients with pancreatic ductal adenocarcinoma. *Cancer Sci* 2017; **108**: 2122-2129 [PMID: 28898495 DOI: 10.1111/cas.13396]

15   **Shiba D**, Terayama M, Yamada K, Hagiwara T, Oyama C, Tamura-Nakano M, Igari T, Yokoi C, Soma D, Nohara K, Yamashita S, Dohi T, Kawamura YI. Clinicopathological significance of cystatin A expression in progression of esophageal squamous cell carcinoma. *Medicine (Baltimore)* 2018; **97**: e0357 [PMID: 29642180 DOI: 10.1097/MD.0000000000010357]

16   **Butler MW**, Fukui T, Salit J, Shaykhiev R, Mezey JG, Hackett NR, Crystal RG. Modulation of cystatin A expression in human airway epithelium related to genotype, smoking, COPD, and lung cancer. *Cancer Res* 2011; **71**: 2572-2581 [PMID: 21325429 DOI: 10.1158/0008-5472.CAN-10-2046]

17   **Lin YY**, Chen ZW, Lin ZP, Lin LB, Yang XM, Xu LY, Xie Q. Tissue Levels of Stefin A and Stefin B in Hepatocellular Carcinoma. *Anat Rec (Hoboken)* 2016; **299**: 428-438 [PMID: 26753874 DOI: 10.1002/ar.23311]

18   **Chang KP**, Wu CC, Chen HC, Chen SJ, Peng PH, Tsang NM, Lee LY, Liu SC, Liang Y, Lee YS, Hao SP, Chang YS, Yu JS. Identification of candidate nasopharyngeal carcinoma serum biomarkers by cancer cell secretome and tissue transcriptome analysis: potential usage of cystatin A for predicting nodal stage and poor prognosis. *Proteomics* 2010; **10**: 2644-2660 [PMID: 20461718 DOI: 10.1002/pmic.200900620]

19   **Takahashi H**, Honma M, Ishida-Yamamoto A, Namikawa K, Kiyama H, Iizuka H. Expression of human cystatin A by keratinocytes is positively regulated *via* the Ras/MEKK1/MKK7/JNK signal transduction pathway but negatively regulated *via* the Ras/Raf-1/MEK1/ERK pathway. *J Biol Chem* 2001; **276**: 36632-36638 [PMID: 11451947 DOI: 10.1074/jbc.m102021200]

20   **Cao X**, Li Y, Luo RZ, Zhang L, Zhang SL, Zeng J, Han YJ, Wen ZS. Expression of Cystatin SN significantly correlates with recurrence, metastasis, and survival duration in surgically resected non-small cell lung cancer patients. *Sci Rep* 2015; **5**: 8230 [PMID: 25648368 DOI: 10.1038/srep08230]

21   **Jiang J**, Liu HL, Liu ZH, Tan SW, Wu B. Identification of cystatin SN as a novel biomarker for pancreatic cancer. *Tumour Biol* 2015; **36**: 3903-3910 [PMID: 25577248 DOI: 10.1007/s13277-014-3033-3]

22   **Cui Y**, Sun D, Song R, Zhang S, Liu X, Wang Y, Meng F, Lan Y, Han J, Pan S, Liang S, Zhang B, Guo H, Liu Y, Lu Z, Liu L. Upregulation of cystatin SN promotes hepatocellular carcinoma progression and predicts a poor prognosis. *J Cell Physiol* 2019; **234**: 22623-22634 [PMID: 31106426 DOI: 10.1002/jcp.28828]

23   **Dai DN**, Li Y, Chen B, Du Y, Li SB, Lu SX, Zhao ZP, Zhou AJ, Xue N, Xia TL, Zeng MS, Zhong Q, Wei WD. Elevated expression of CST1 promotes breast cancer progression and predicts a poor prognosis. *J Mol Med (Berl)* 2017; **95**: 873-886 [PMID: 28523467 DOI: 10.1007/s00109-017-1537-1]

24   **Jiang J**, Liu HL, Tao L, Lin XY, Yang YD, Tan SW, Wu B. Let7d inhibits colorectal cancer cell proliferation through the CST1/p65 pathway. *Int J Oncol* 2018; **53**: 781-790 [PMID: 29845224 DOI: 10.3892/ijo.2018.4419]

25   **Yoneda K**, Iida H, Endo H, Hosono K, Akiyama T, Takahashi H, Inamori M, Abe Y, Yoneda M, Fujita K, Kato S, Nozaki Y, Ichikawa Y, Uozaki H, Fukayama M, Shimamura T, Kodama T, Aburatani H, Miyazawa C, Ishii K, Hosomi N, Sagara M, Takahashi M, Ike H, Saito H, Kusakabe A, Nakajima A. Identification of Cystatin SN as a novel tumor marker for colorectal cancer. *Int J Oncol* 2009; **35**: 33-40 [PMID: 19513549 DOI: 10.3892/ijo_00000310]

26   **Choi EH**, Kim JT, Kim JH, Kim SY, Song EY, Kim JW, Yeom YI, Kim IH, Lee HG. Upregulation of the cysteine protease inhibitor, cystatin SN, contributes to cell proliferation and cathepsin inhibition in gastric cancer. *Clin Chim Acta* 2009; **406**: 45-51 [PMID: 19463800 DOI: 10.1016/j.cca.2009.05.008]

27   **Hong J**, Hu K, Yuan Y, Sang Y, Bu Q, Chen G, Yang L, Li B, Huang P, Chen D, Liang Y, Zhang R, Pan J, Zeng YX, Kang T. CHK1 targets spleen tyrosine kinase (L) for proteolysis in hepatocellular carcinoma. *J Clin Invest* 2012; **122**: 2165-2175 [PMID: 22585575 DOI: 10.1172/JCI61380]

28   **Xu S**, Wu Y, Chen Q, Cao J, Hu K, Tang J, Sang Y, Lai F, Wang L, Zhang R, Li SP, Zeng YX, Yin Y, Kang T. hSSB1 regulates both the stability and the transcriptional activity of p53. *Cell Res* 2013; **23**: 423-435 [PMID: 23184057 DOI: 10.1038/cr.2012.162]

29   **Lu J**, Li Y, Wu Y, Zhou S, Duan C, Dong Z, Kang T, Tang F. MICAL2 Mediates p53 Ubiquitin Degradation through Oxidating p53 Methionine 40 and 160 and Promotes Colorectal Cancer Malignance. *Theranostics* 2018; **8**: 5289-5306 [PMID: 30555547 DOI: 10.7150/thno.28228]

30   **Tang FQ**, Duan CJ, Huang DM, Wang WW, Xie CL, Meng JJ, Wang L, Jiang HY, Feng DY, Wu SH, Gu HH, Li MY, Deng FL, Gong ZJ, Zhou H, Xu YH, Tan C, Zhang X, Cao Y. HSP70 and mucin 5B: novel protein targets of N,N'-dinitrosopiperazine-induced nasopharyngeal tumorigenesis. *Cancer Sci* 2009; **100**: 216-224 [PMID: 19068094 DOI: 10.1111/j.1349-7006.2008.01028.x]

31   **Tang F**, Zou F, Peng Z, Huang D, Wu Y, Chen Y, Duan C, Cao Y, Mei W, Tang X, Dong Z. N,N'-dinitrosopiperazine-mediated ezrin protein phosphorylation *via* activation of Rho kinase and protein kinase C is involved in metastasis of nasopharyngeal carcinoma 6-10B cells. *J Biol Chem* 2011; **286**: 36956-36967 [PMID: 21878630 DOI: 10.1074/jbc.M111.259234]

32   **Birkenmeier EH**, Brown DD, Jordan E. A nuclear extract of Xenopus laevis oocytes that accurately transcribes 5S RNA genes. *Cell* 1978; **15**: 1077-1086 [PMID: 569551 DOI: 10.1016/0092-8674(78)90291-x]

33   **Abascal-Palacios G**, Ramsay EP, Beuron F, Morris E, Vannini A. Structural basis of RNA polymerase III transcription initiation. *Nature* 2018; **553**: 301-306 [PMID: 29345637 DOI: 10.1038/nature25441]

34   **Yeganeh M**, Hernandez N. RNA polymerase III transcription as a disease factor. *Genes Dev* 2020; **34**: 865-882 [PMID: 32611613 DOI: 10.1101/gad.333989.119]

35   **Ramsay EP**, Abascal-Palacios G, Daiß JL, King H, Gouge J, Pilsl M, Beuron F, Morris E, Gunkel P, Engel C, Vannini A. Structure of human RNA polymerase III. *Nat Commun* 2020; **11**: 6409 [PMID: 33335104 DOI: 10.1038/s41467-020-20262-5]

36   **Cabarcas S**, Schramm L. RNA polymerase III transcription in cancer: the BRF2 connection. *Mol Cancer* 2011; **10**: 47 [PMID: 21518452 DOI: 10.1186/1476-4598-10-47]

37   **Lei J**, Chen S, Zhong S. Abnormal expression of TFIIIB subunits and RNA Pol III genes is associated with hepatocellular carcinoma. *Liver Res* 2017; **1**: 112-120 [PMID: 29276645 DOI: 10.1016/j.livres.2017.08.005]

38   **Zhong Q**, Xi S, Liang J, Shi G, Huang Y, Zhang Y, Levy D, Zhong S. The significance of Brf1 overexpression in human hepatocellular carcinoma. *Oncotarget* 2016; **7**: 6243-6254 [PMID: 26701855 DOI: 10.18632/oncotarget.6668]

39   **Bellido F**, Sowada N, Mur P, Lázaro C, Pons T, Valdés-Mas R, Pineda M, Aiza G, Iglesias S, Soto JL, Urioste M, Caldés T, Balbín M, Blay P, Rueda D, Durán M, Valencia A, Moreno V, Brunet J, Blanco I, Navarro M, Calin GA, Borck G, Puente XS, Capellá G, Valle L. Association Between Germline Mutations in BRF1, a Subunit of the RNA Polymerase III Transcription Complex, and Hereditary Colorectal Cancer. *Gastroenterology* 2018; **154**: 181-194.e20 [PMID: 28912018

DOI: 10.1053/j.gastro.2017.09.005]

40   **Gouge J**, Guthertz N, Kramm K, Dergai O, Abascal-Palacios G, Satia K, Cousin P, Hernandez N, Grohmann D, Vannini A. Molecular mechanisms of Bdp1 in TFIIIB assembly and RNA polymerase III transcription initiation. *Nat Commun* 2017; **8**: 130 [PMID: 28743884 DOI: 10.1038/s41467-017-00126-1]

41   **Georgakopoulos-Soares I**, Chartoumpekis DV, Kyriazopoulou V, Zaravinos A. EMT Factors and Metabolic Pathways in Cancer. *Front Oncol* 2020; **10**: 499 [PMID: 32318352 DOI: 10.3389/fonc.2020.00499]